Direct Observation of Ylide and Enol Intermediates Formed in Competition with Wolff Rearrangement of Photo-Excited Ethyl Diazoacetoacetate

Ryan Phelps and Andrew J. Orr-Ewing*

School of Chemistry, University of Bristol, Cantock's Close, Bristol BS8 1TS, UK

* Author for correspondence. E-mail: a.orr-ewing@bristol.ac.uk

Abstract

The photoexcitation of α-diazocarbonyl compounds produces ketenes by both concerted and stepwise Wolff rearrangements. The stepwise mechanism proceeds through singlet carbene intermediates which can also participate in bimolecular reactions such as ylide formation with nucleophiles. Here, ultrafast transient infra-red absorption spectroscopy is used to show competitive production of singlet carbene and ketene intermediates from the photoexcitation of ethyl diazoacetoacetate. We provide direct spectroscopic evidence for ylide formation by singlet α-carbonyl carbene capture in aprotic nucleophilic solvents (with ylide bands at 1625 cm^{-1} in acetonitrile, and 1586 cm^{-1} and 1635 cm^{-1} in tetrahydrofuran) and report an enol mediated pathway for singlet α-carbonyl carbene reaction with alcohols (ethanol or t-butanol) identified by an absorption band at 1694 cm^{-1}, but find no evidence for a previously proposed ylide pathway. The α-carbonyl carbene is monitored using a band with solvent-dependent wavenumber in the range 1627 – 1645 cm^{-1}. A computed two-dimensional cut of the potential energy surface for the reaction of the singlet α-carbonyl carbene with methanol shows that the enol forms without a barrier, and that this reaction is promoted by an intermolecular hydrogen bond from methanol to the carbonyl oxygen atom. The corresponding ylide structure lies higher in energy, with a barrierless downhill path to isomerization to the enol.

1. Introduction

The ketene-forming Wolff rearrangement (WR) of photo-excited α-diazocarbonyl compounds can follow either concerted or stepwise pathways, the latter via singlet carbonyl carbene intermediates which may also undergo competing reactions (Scheme 1). This photochemical rearrangement is used in a range of synthetic processes including ring contractions[1-2] and the Arndt-Eistert synthesis of carboxylic acids.[3] However, direct observations of the carbenes, and of other proposed intermediates in their reactions, remain rare because of their high reactivity and hence short lifetimes.

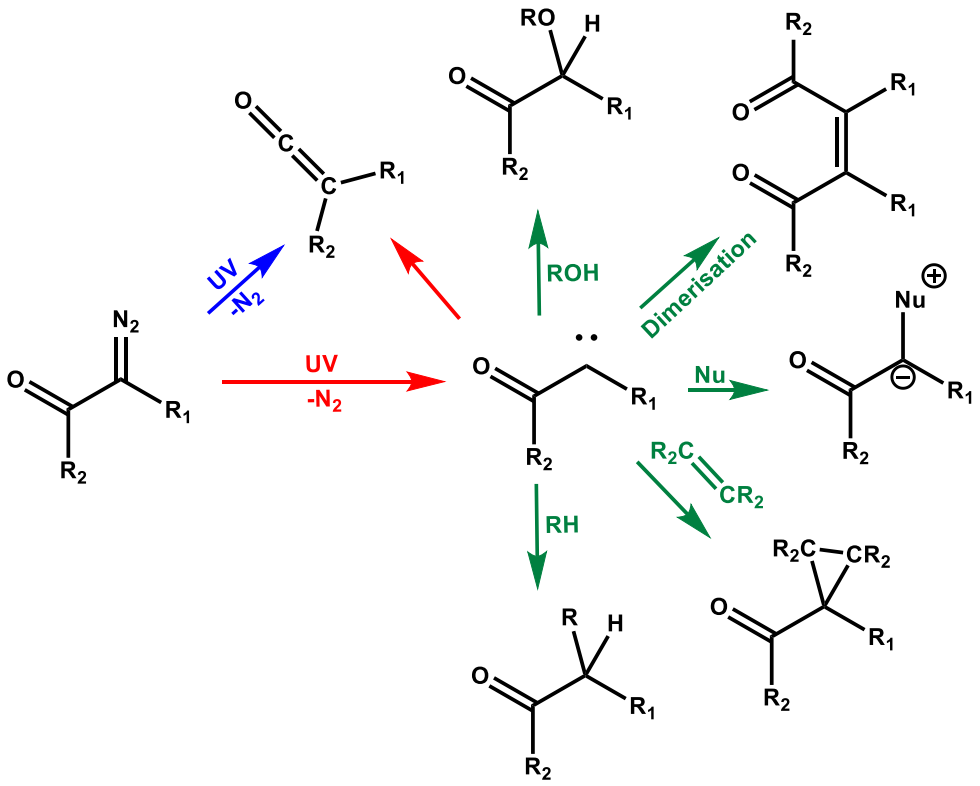

Scheme 1 – UV photoexcitation of α-diazocarbonyl compounds to produce singlet carbonyl carbenes and ketene intermediates. Arrows indicate concerted (blue) and stepwise (red) Wolff-rearrangements, and possible competing reactions of the singlet carbene (green).

One notable example of observation of these reactive intermediates is the report by Platz and co-workers of transient absorption spectroscopy (TAS) measurements with infrared (IR) and ultraviolet (UV) probe wavelengths following the photoexcitation of the α-diazocarbonyl compound azibenzil in acetonitrile (ACN). WR was shown to occur on ultrafast (<0.3 ps) and slower (700 ps) timescales by monitoring the product ketene stretching mode at 2113 cm^{-1}, consistent with contributions from both the concerted and stepwise WR pathways after photoexcitation. This interpretation was supported by the observed kinetics of a near-UV transient absorption band at 370 nm which was assigned to the singlet carbene.[4] Platz and co-workers found further evidence for a singlet carbene to ketene transformation in the photoexcitation of p-biphenylyl diazo ketone. The observed lifetime of the singlet carbene depended on the solvent, with ACN and tetrahydrofuran (THF) argued to stabilise the singlet carbene and suppress WR. In contrast, in methanol (MeOH) a shorter singlet carbene lifetime was postulated to be a consequence of reaction with the solvent in competition with Wolff rearrangement, but reaction products were not assigned.[5]

α-Diazocarbonyl compounds typically adopt locally planar geometries, and the partial double C-C bond character results in syn and anti-isomers.[6] Experimental evidence points to selectivity towards the concerted and stepwise Wolff rearrangements from the syn and anti-isomers respectively.[7] For example, photo-excited methyl 2-diazo-(2-naphthyl) acetate, 99% of which adopts an anti-form, undergoes only the stepwise WR,[8 9] whereas the cyclic diazo-compounds diazonaphthoquinone (DNQ) and 5-diazomeldrum acid (DMA), which are locked in their syn-isomers, favour concerted Wolff rearrangement.[10-11]

Computational methods have further explored the proposed mechanisms for the Wolff rearrangement using electronically non-adiabatic trajectory simulations. In these calculations, $S_2 \leftarrow S_0$ ($\pi^* \leftarrow \pi$) photo-excited DNQ showed rapid internal conversion to the S_1 state (with π^*character localized on the diazo group), where C-N extension brought the molecule to an S_1/S_0 conical intersection.[12] After ultrafast decay to the S_0 state through this intersection, the C-N coordinate continued to extend to form a hot singlet carbene that either vibrationally cooled or rearranged to a ketene within ~10 ps. A competing pathway to ketene formation involving simultaneous C-C shortening and C-N elongation indicated concerted WR within 400 fs. Recent non-adiabatic trajectory calculations for photo-excited DMA identified similar mechanisms for WR as well as an S_1 pathway to singlet carbene formation.[13] The stepwise Wolff rearrangement in DMA happened within 500 fs, which is consistent with previous reports.[10]

The extent to which Wolff rearrangement occurs is influenced by the nature of the migratory group.[14] Here, we focus on the effect alkoxy groups have on the propensity for WR. In prior experimental studies of diazo-3-ketocaboxylates, the ester functionality was found not to migrate.[15-16] These conclusions derived from stable product analysis, but ultrafast time resolved spectroscopy offers direct observation of the reaction pathways. For example, photoexcitation of a biphenyl diazo ester produced a singlet carbene, with no evidence for Wolff rearrangement,[5] in contrast with the keto-derivative where both stepwise and concerted WR pathways were active.[17] The reluctance of alkoxy groups to migrate via WR is likely to be a consequence of higher activation barriers because of the energy required to break the ester resonance.[5]

In the presence of alcohols, ethers, nitriles or other nucleophiles, singlet carbenes react to form ylides. Direct observation of ACN ylides has been reported in a low-temperature matrix,[18] but most evidence of ylide formation under ambient conditions is inferred from the reaction products. Exceptions include the use of time resolved infra-red (TRIR) spectroscopy to reveal spectral bands of intermediates from the photoexcitation of ethyl diazoacetate in ACN, one of which was attributed to an ylide on the basis of calculated vibrational mode frequencies.[19] Further such observations of ACN and dioxane derived

ylides have also been reported.[19-20] The mechanisms by which singlet carbenes react with alcohols to make ethers are thought to follow the three pathways shown in Scheme 2, with their relative significance depending on the electron donating or withdrawing character of R_1 and R_2 substituents.[21] Carbocation intermediates of the protonation of diphenylcarbene were previously identified by TAS with a probe spanning the near-UV and visible regions,[22-23] but the formation of the alcohol-ylide intermediate species has received less attention. Xue *et al*. presented direct evidence for an alcohol ylide, in this case from reaction of singlet carboethoxycarbene,[19] but used an ester carbene to suppress WR. Hence, any competition between WR and bimolecular reaction pathways was not examined.

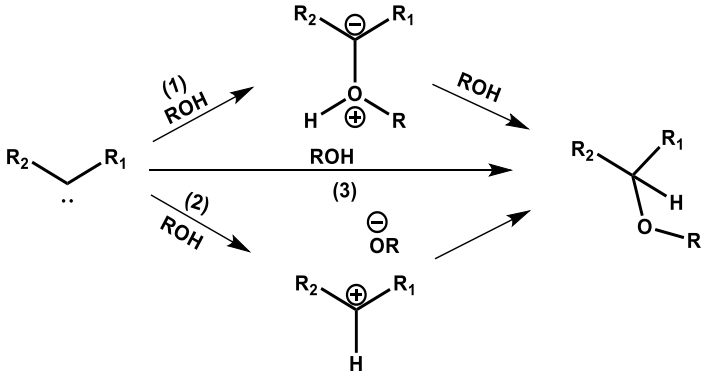

Scheme 2 – Proposed pathways for singlet carbene reaction with an alcohol to make an ether. For α-carbonyl carbenes, a further reaction pathway with H_2O forming an enol product is shown in Scheme 3.

Both the ylide (path 1) and carbocation (path 2) intermediate pathways shown in scheme 2 are widely accepted,[24] although in the 1960s Strausz *et al*. proposed the formation of an enol intermediate in carbonyl carbene – alcohol reactions.[25] This idea of carbonyl involvement was revisited in the 1990s by Platz and co-workers, but they preferred to assign a transient electronic absorption band to an ylide structure.[26] Evidence has been presented of enol formation by carbonyl carbene insertion into O-H bonds of H_2O (Scheme 3),[27-28] but this mode of reactivity has yet to be demonstrated for alcohols.

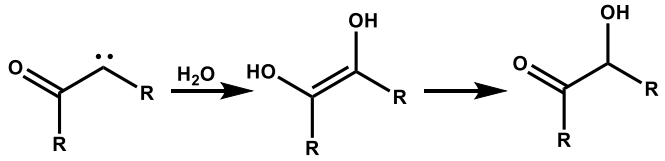

Scheme 3 – Reaction of H_2O with a singlet carbonyl carbene to produce an enol intermediate.

Here, we provide direct evidence from TRIR measurements for singlet carbonyl carbene formation and reaction in competition with concerted WR of a UV photo-excited α-diazo carbonyl compound, ethyl diazoacetoacetate (EDAA). Furthermore, we report the competitive formation of a previously unobserved alcohol-derived enol as an intermediate to ether formation, and we compare the nucleophilic reactivity of the singlet carbene in a range of solvents.

2. Method

A. Experiment. The photoinduced chemistry of ethyl diazoacetoacetate was studied in cyclohexane and several nucleophilic solvents using TRIR with a broadband IR probe. Spectra were collected following the photoexcitation at 256 nm of 3.2 mM samples of EDAA (Sigma Aldrich, ≤100%) used as received. At this UV wavelength, absorption is assigned to the $S_4 \leftarrow S_0$ excitation, orbital contributions for which are shown in figure S12 of the Supporting Information. With a sample path length of 380 μm, an absorbance at 256 nm of approximately 0.6 was obtained. Measurements were made for EDAA solutions in cyclohexane (Fisher Scientific, extra pure, SLR grade), tetrahydrofuran (Fisher Scientific, extra pure, SLR grade, stabilised with 0.025% BHT), acetonitrile (Fisher Scientific, HPLC gradient grade, <99.9%), ethanol ((EtOH) Sigma Aldrich, ACS reagent grade, >99.5%), and tertiary butanol ((t-BuOH) Sigma Aldrich, anhydrous, ≥99.5%). Steady-state FTIR and UV absorption spectra for these EDAA solutions are shown in figures S10 and S11 of the Supporting Information.

The instrumental set-up has been described in detail elsewhere.[29] In brief, a Coherent Vitara-S oscillator and Coherent Legend Elite HE+ regenerative amplifier operating at 1 kHz generated 800 nm pump pulses with a 40 fs duration and a maximum total output power of 5 W. The pump beam was divided using a series of beam splitters to provide two beams at a maximum of 2.45 mJ/pulse. These two beams seeded Coherent OPerA Solo optical parametric amplifiers (OPAs). One OPA generated tuneable UV pump pulses, and the other produced broadband (~300 cm^{-1}) mid-IR probe pulses. The IR probe was focused onto the sample using a concave aluminium mirror and overlapped with a UV pump pulse, which was focused onto the sample using a CaF_2 lens (f = 200 mm). The beam diameter of the pump pulse was set to be larger than that for the probe to excite uniformly the probed sample region.

The temporal delay between the pump and probe pulses was controlled using a motorised 22-cm delay stage (Thorlabs DDS220/M), which provided a maximum delay of 1.3 ns. A mechanical chopper (Thorlabs, MC2000) intersected the pump pulse at a repetition rate of 500 Hz to collect pump-on and pump-off spectra with alternate probe laser pulses, from which pump-induced difference spectra were derived. Measurements were made in a Harrick cell assembled from two 1.5-mm thick CaF_2 windows

separated by 380-µm Teflon spacers, with the sample circulating constantly from a 25-ml reservoir to avoid photodegradation. All spectra were obtained under aerobic conditions, with dissolved oxygen only expected to affect the photochemistry on timescales >100 ns that are much longer than the temporal window probed.[30] After passing through the sample, the IR probe pulses were directed into a spectrometer (HORIBA Scientific, iHR320) fitted with a 128-element, liquid nitrogen cooled Mercury Cadmium Telluride array (Infrared Associates Inc., MCT-10−128) and fast read-out electronics (Infrared Systems Development Corp, FPAS-0144), giving a spectral resolution of 2 cm^{-1} per pixel for spectra acquired around 1650 cm^{-1} and 3 cm^{-1} per pixel in the 2100 cm^{-1} region. A portion of the IR beam was split off from the probe beam pathway before the sample and passed to a reference spectrometer of matching configuration.

B. Computational details. Assignments of transient IR bands were supported by gas phase anharmonically corrected vibrational frequencies computed with density functional theory (DFT). These calculations used the B3LYP functional and the 6-311++G(d,p) basis set for all the species considered in this study. Accurate geometries[31] and anharmonically corrected vibrational frequencies[32-33] of organic molecules have been reported using this chosen level of theory. Calculations achieved respective accuracies within 9 cm^{-1} and 33 cm^{-1} in reproducing experimental ketone and ester carbonyl stretching frequencies for EDAA in all the solvents studied. A solvent correction in the form of the polarisable continuum model (PCM) can lead to erronous results with anharmonic frequency calculations,[34] and was not applied. Because of the accuracy of the calculated carbonyl stretching band wavenumbers, detection and assignment of transient intermediates largely relied on comparisons of experimental measurements and computational simulation of bands observed in this spectral window. Comparisons with measured spectra in the ketene stretching region around 2100 cm^{-1} provided further evidence for certain product pathways. Proposed assignments were also supported by experimentally derived kinetic data and computed energies of intermediates and products.

To provide further understanding of the mechanism of singlet carbene insertion into alcohols, relaxed potential energy scans were calculated at the B3LYP/6-311++G(d,p) level to map out the potential energy surface for reaction of MeOH with the EDAA-derived singlet carbene. In these scans, two coordinates were varied and all other geometric parameters were relaxed. The two coordinates chosen were the distance of the oxygen atom of MeOH from the carbene carbon atom, which was incremented over 175 steps with a stepsize of 0.01 Å, and the MeOH O-H distance which was increased with a stepsize of 0.05 Å over 10 steps. All calculations were performed for species in the gas phase using the Gaussian 09 computational package.[35]

4. Results and Discussion

Scheme 4 serves as a guide for our discussion of the observed photochemical pathways of EDAA in a range of solvents. At equilibrium, EDAA exists in 4 different isomers, with calculated gas-phase Gibbs energies (see Table S2 of the Supporting Information) that show 87 % exists as the Z,E-isomer (shown as (1) in scheme 4). The photolysis of EDAA (1) is expected to retain this stereochemistry, forming the more stable anti-isomer of the carbene (shown as (2) in scheme 4). Conjugation of the carbene lone pair of electrons into the α-carbonyl groups hinders internal rotation, preventing rearrangement to other carbene stereoisomers. Similar arguments apply to the isomers of potential reaction products, as is discussed further below.

We begin with IR bands associated with the primary photoproducts observed in non-reactive cyclohexane, and we then identify alternative photochemical channels that arise in various nucleophilic solvents. Summaries of the observed band positions and measured time constants for the various intermediates are presented respectively in Table 1 and Table S1 (Supporting Information). We found no evidence for triplet carbene participation in any of our experiments, consistent with computational prediction of a singlet carbene ground state for species (2). Reference to carbenes hereafter thus implies only the singlet species.

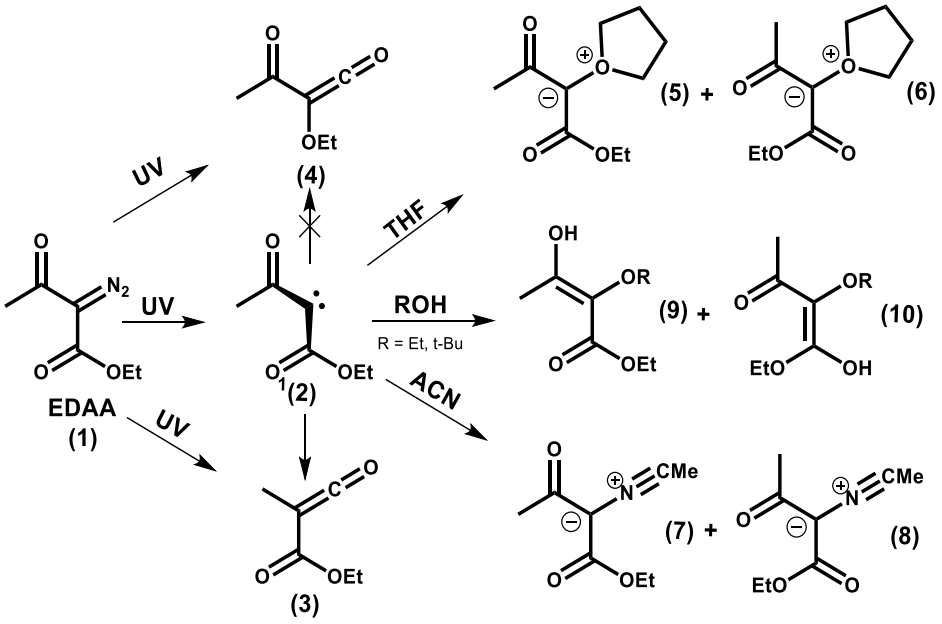

Scheme 4 – The photochemical pathways of EDAA in solution determined by transient vibrational absorption spectroscopy. Carbene (2) has a singlet ground-state, emphasized here by the ^{1}(2) notation.

Table 1 – Band Positions of the Intermediates Observed in the Five Solvents Studied. Intermediates are Identified by Bold Numbers in Parentheses Corresponding to the Labels Used in Scheme 4.

	Cyclohexane (cm^{-1})	THF (cm^{-1})	ACN (cm^{-1})	EtOH (cm^{-1})	t-BuOH (cm^{-1})
Ketene (**3**)	2125	2130	2130	2130	2130
	1722	1715	1711	1720	1722
Ketene (**4**)	2105				
Carbene (**2**)	1645	1646	1627		1636
Ylide		1586 (**5**)	1625 (**7**)		
		1635 (**6**)			
Enol (**9**)				1694	1694

4.1 Wolff rearrangement

Figures 1 and 2 show TRIR spectra, obtained in two different probe wavenumber regions, for the photoexcitation of EDAA in a variety of solvents. Negative-going bands centred around 2130 cm^{-1} (diazo stretch) (Figure 1(a)), and 1670 cm^{-1} (ketone stretch) and 1730 cm^{-1} (ester stretch) (Figure 2(a)) in cyclohexane are assigned to ground state bleaches (GSB) of EDAA vibrational bands on the basis of steady-state IR absorption spectra. A 15% GSB recovery of the 1670 cm^{-1} band implies 85% conversion of photo-excited EDAA to photoproducts. Regeneration of ground state EDAA can therefore be discounted as the only cause of the observed 50-75% recovery in the 1730 cm^{-1} and 2130 cm^{-1} GSBs, which must instead be a result of overlapping photoproduct bands. Data-fitting to decompose these bands into their overlapping components is shown in Figure S8 and Figure S9 of the Supporting Information.

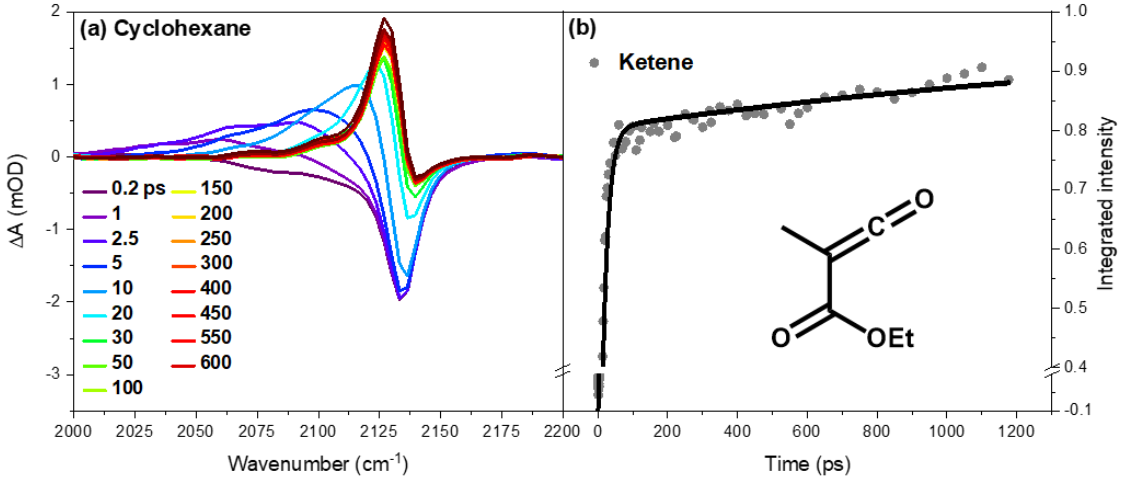

Figure 1 – Photoinduced ketene formation from EDAA: (a) TRIR spectra for the 256-nm photoexcitation of EDAA in cyclohexane. Spectra were obtained by monitoring the C=C=O ketene stretching region from 2000 – 2200 cm^{-1}. The inset key shows the colour scheme identifying transient spectra obtained at

different time delays after the UV excitation laser pulse. (b) A kinetic fit to the growth of integrated intensity of the 2125 cm^{-1} band corresponding to a vibrationally cooled ground-state ketene. The inset structure shows our preferred assignment of the 2125 cm^{-1} band to ketene (3). Grey circles are experimental measurements and the solid line is a fit to a biexponential function giving time constants of 17 ± 1 ps and >1 ns.

Table 2 – Time Constants for the Production of Ketene (3) after UV Photoexcitation of EDAA in Various Solvents, and Percentage Contributions of the Stepwise WR.

Solvent	τ_1/ ps	τ_2/ ps	Stepwise WR fraction / %
Cyclohexane	17 ± 1	> 1000	20 ± 8
ACN	15.7 ± 0.6	≈ 1000	4 ± 2
THF	11.5 ± 0.3	180 ± 100	4 ± 2
EtOH	11.0 ± 0.3		0
t-BuOH	10.9 ± 0.4		0

EDAA has two carbonyl groups adjacent to the diazo group (i.e. in α positions), and two alternative WR reactions are therefore possible, as shown in Scheme 4. Rearrangement involving the ketone functionality yields ketene (3), whereas rearrangement of the ester functionality produces ketene (4). Ketene photoproducts are unambiguously identified by monitoring the characteristic IR bands associated with the C=C=O stretching modes and indicate two isomers with bands at 2125 and 2105 cm^{-1} in cyclohexane (Figure 1(a)). The ketene molecules are born within the instrument response time (i.e. < 300 fs) and with excess vibrational energy, as is evident from the breadth of the bands at early times and their narrowing and shift to higher wavenumber with increasing time delay as excess internal energy dissipates to the solvent. The prompt ketene formation is consistent with a concerted WR reaction. A further long-term growth in intensity is observed for the 2125 cm^{-1} band (Figure 1(b) and Supporting Information, Figure S3) over time-delays extending to beyond 1 ns, which suggests a contribution to the ketene yield from the stepwise WR and hence the participation of carbene intermediates.

Similar observations of ketene formation were made in all our chosen nucleophilic solvents (see Supporting Information, Figure S1). Time constants associated with the growth of the 2125 cm^{-1} band, as well as the percentage contribution from the stepwise WR, are summarized in Table 2. The faster of the two observed time constants is attributed to the dynamics of vibrational cooling of promptly formed hot ketene molecules after concerted WR, with the longer time constant a direct measure of the product ketene growth associated with the stepwise WR. The observed suppression of the stepwise WR in

nucleophilic solvents results from solvent molecules intercepting the carbene intermediates before this WR pathway can occur. We were unable to perform a kinetic analysis at early times (<20 ps) for the weaker 2105 cm^{-1} band because of overlap by the broad absorption associated with vibrationally hot ketene molecules. However, no detectable long-term growth of the 2105 cm^{-1} band implies that stepwise WR does not occur for the associated ketene on these time scales (Supporting Information, Figure S3).

Computations of single point energies and transition states identify that ketene (3) lies 113 kJ mol^{-1} below ketene (4) in energy, and the former has a 13.7 kJ mol^{-1} lower activation energy for formation from the intermediate carbene (2) (shown in table S5 of supporting information). These arguments favour ketene (3) as the product of the stepwise WR pathway, hence the 2125 cm^{-1} band is assigned to it, with ketene (4) proposed to be responsible for the band around 2105 cm^{-1}. These assignments are consistent with vibrational frequency calculations that predict ketene stretching frequencies to be higher for product (3) than for product (4).

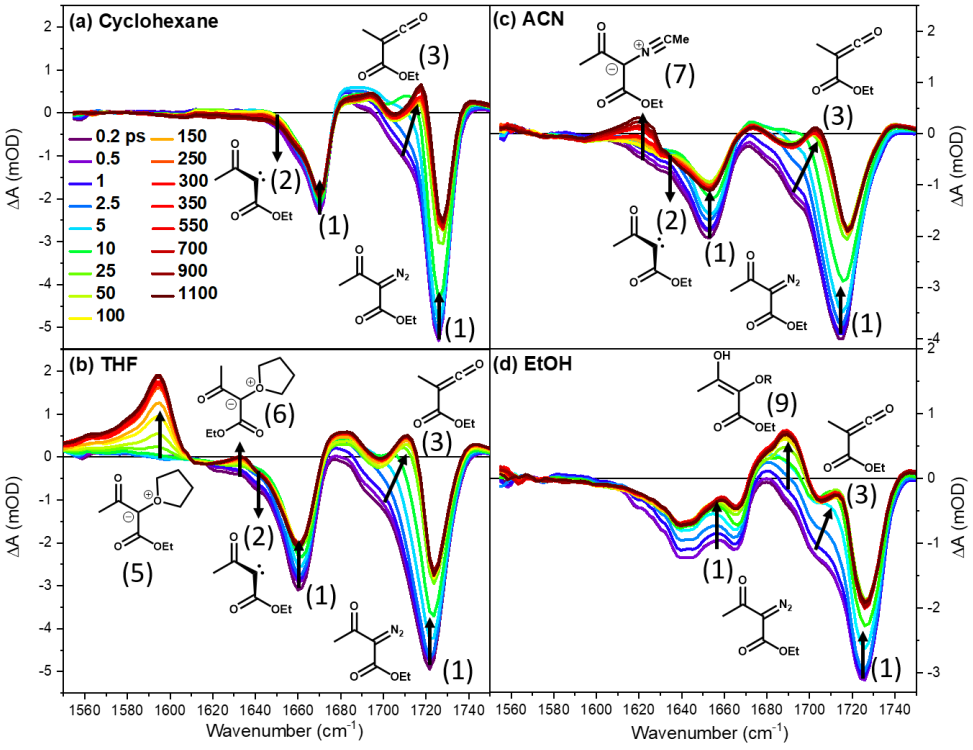

Figure 2 – Spectroscopic evidence for various intermediates from carbene reactions in different solvents. TRIR spectra are shown for 3.2 mM EDAA solutions after photoexcitation at 256 nm. The solvents used are (a) cyclohexane; (b) THF; (c) ACN; (d) EtOH. The inset colour key in panel (a) identifies spectra obtained at different time delays, and black arrows show the directions of change of spectral features with time. Numbers in parentheses provide band assignments to structures in Scheme 4.

A positive-going band indicative of photoproducts is centred between 1700 and 1725 cm^{-1} but overlaps the EDAA parent molecule GSB (e.g. Figure 2(a)). This band is observed both in the unreactive cyclohexane solvent and in all the nucleophilic solvents studied. The associated photoproduct is born vibrationally hot and undergoes vibrational cooling, as shown by the band narrowing and shifting to higher wavenumber with increasing time delay. The band is further found to increase over longer times in cyclohexane, ACN, and THF. For the alcohol solvents studied, after its initial rise the band intensity remains constant for the duration of the experiment. Assignment of this band to carbene (2) can be discounted because it does not decay by reaction with nucleophilic solvents or stepwise WR. Photoisomerization of EDAA to a diazirine could account for the prompt band appearance, with predicted product vibrational frequencies of 1725 and 1740 cm^{-1}, but this does not explain the long-term growth of the band. A more plausible assignment is to ketene (3), which has a predicted vibrational band at 1732 cm^{-1} (ester stretch), because the kinetics of growth of the 1725 cm^{-1} band at longer time delays match those of the ketene band at 2125 cm^{-1} in all solvents.

4.2 Ylide formation

To investigate the photoinduced reactions of singlet carbenes with nucleophiles and the possible generation of ylide intermediates, we performed TRIR measurements for EDAA solutions in THF and ACN. These solvents were chosen in part because they contain no acidic hydrogen atoms, hence ruling out formation of carbocation intermediates of the type shown in Scheme 2. Transient IR bands associated with ylide intermediates and insertion reaction products are therefore more readily identified.

Bands centred at 1586 cm^{-1} in THF (figure 2(b)) and 1625 cm^{-1} in ACN (figure 2(c)) are assigned to the respective ylides (5) and (7) in Scheme 4, based upon good agreement with calculated vibrational frequencies of the ketone stretching modes at 1564 cm^{-1} and 1634 cm^{-1} respectively. An additional weaker band in THF at 1635 cm^{-1} is assigned to the E,Z-isomer (6), which is formed when the THF molecule approaches the carbonyl anti to the ketone functionality. Isomer (6) sits 32.4 kJ mol^{-1} higher in energy (see Table S4 of Supporting Information) and is therefore expected to be a minor contributor. The ylides are formed with time constants of 140 ± 6 ps in THF, and ≈ 1 ns in ACN by solvent nucleophilic attack at the carbene centre. The lifetimes of the ylides are longer than the 1.3-ns time limit of our experiment. The E,Z-isomer of the ACN ylide (8) has a predicted IR band at 1653 cm^{-1} which is likely to overlap other bands

in the transient spectra. This isomer is also expected to be only a minor product on energetic grounds, and it remains unassigned in our measured spectra.

The observation of ylides provides further evidence for carbene (2) production by photoexcitation of EDAA, and hence for competition between photoinduced carbene formation and concerted WR pathways. TRIR measurements for EDAA in alcohol solutions do not show such clear-cut evidence for ylide bands in our probe spectral window, and alternative reaction pathways are discussed in section 4.3.

4.3 Enol formation

For photo-excited solutions of EDAA in EtOH, a transient absorption band identified at 1694 cm^{-1} has a 35 ± 2 ps time constant for growth (figure 2(d)). A similar feature is observed for EDAA in t-BuOH with a corresponding time constant of 160 ± 30 ps (see Figure S4 of Supporting Information). Calculated vibrational frequencies for the alcohol ylide suggest bands should be observable at 1598 cm^{-1} and 1736 cm^{-1}, i.e. at the lower and upper edges of the spectral regions shown in Figure 2, but we were unable to detect any such bands close to the predicted features in measurements covering 1550 - 1800 cm^{-1}. We argue against the assignment of the 1694 cm^{-1} band to an alcohol ylide because the discrepancies with the bands computed to appear at 1598 cm^{-1} (a ketone stretch) and 1736 cm^{-1}, both assigned to isomer 2 in Table S7 of Supporting Information, lie outside the level of agreement with computational predictions demonstrated for ylide bands in THF and ACN. Solvation of the EtOH ylide might account for a significant shift to lower wavenumber than the predicted 1736 cm^{-1} band position. However, we argue against this proposition because THF ylides formed in THF:EtOH mixtures show no more than -10 cm^{-1} shifts upon displacement of THF by EtOH in the solvation shell of the ylide (see Figure S6 of Supporting Information). For such modest solvent shifts with alcohols, we would also expect to see the absorption band computed to appear at 1598 cm^{-1} in the spectral window covered by our experimental measurements, but it is not observed. Further, indirect arguments against an ylide assignment of the 1694 cm^{-1} band are presented in Figure S6 of Supporting Information.

An alternative assignment is therefore needed for the 1694 cm^{-1} band. A cation absorption (Scheme 2) is ruled out because in this spectral region the only expected band has a predicted wavenumber of 1740 cm^{-1}. Assuming bimolecular reaction with solvent is responsible for the 1694 cm^{-1} band in EtOH solution, the rate of growth identifies an apparently diffusion-controlled reaction rate coefficient. Measurements in cyclohexane:EtOH mixtures of different ratios indicate a rate coefficient k = (4.3 ± 0.3) × 10^{10} dm^3 mol^{-1} s^{-1} (Supporting Information, Figure S5). TRIR measurements in THF:EtOH mixtures reveal direct competition between growth of the 1694 cm^{-1} band and the band identifying the

THF ylide (Supporting Information, Figure S6), confirming that the 1694 cm^{-1} band derives from reaction of carbene (2).

To investigate further the mechanism for the reaction between carbene (2) and alcohols, a two-dimensional relaxed potential energy surface was computed for the reaction with a MeOH molecule. The outcome is shown in Figure 3 and reveals barrierless formation of an enol species, as well as suggesting involvement of one of the carbonyl groups in the reaction. The α-carbonyl group appears to promote the enol pathway by a hydrogen bonding interaction with the alcohol which facilitates a barrierless proton transfer along the intermolecular hydrogen bond. The ylide is computed to lie higher in energy than the enol, and it is connected to the enol by a pathway which is monotonically downhill in potential energy. The pathway to the carbocation is an energetically uphill process that is likely to be inaccessible. Single point energy calculations predict enol (9) to be 146 kJ mol^{-1} more stable than the ylide isomer of the type shown in Scheme 2. Computed vibrational frequencies of the enol identify a strong band at 1713 cm^{-1} (an ester carbonyl stretch) which agrees satisfactorily with the experimentally observed 1694 cm^{-1} feature. For these reasons, the preferred assignment of this band is to enol (9).

Alcohol reaction anti to the ketone functionality of carbene (2) yields enol (10) by a barrierless pathway involving the ester carbonyl group (see Figure S13 of Supporting Information). Enol (10) has a predicted vibrational band at 1694 cm^{-1} (the ketone stretch), but lies 73.8 kJ mol^{-1} higher in energy than enol (9) and is therefore expected to only be a minor contributor to the band intensity. Another solvent dependent band is observed in Figure 2(d) between 1650 and 1670 cm^{-1}, with the EtOH concentration dependence of its growth rate establishing a diffusion-limited rate coefficient consistent with that found for enol (9). Several minima were identified in our theoretical calculations corresponding to different isomers of enol (9). In particular, its Z,Z-isomer (isomer 4, Supporting Information, Table S7) is only 3.3 kJ mol^{-1} higher in energy and forms from the syn-isomer of the carbene. Isomer 4 (Supporting Information, Table S7) has a predicted IR-active mode at 1648 cm^{-1} (ester stretch), making it a plausible candidate for the feature lying between 1650 and 1670 cm^{-1}.

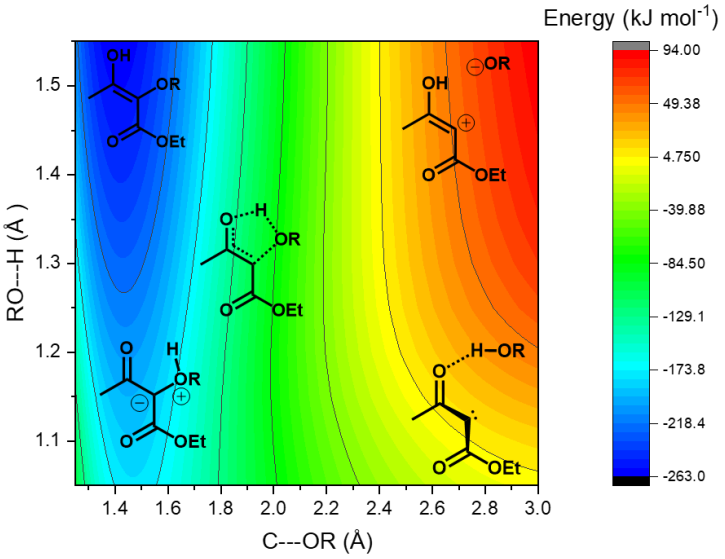

Figure 3 – A computed two-dimensional relaxed potential energy surface showing the minimum energy pathway for the reaction of MeOH with the EDAA-derived carbene (2). The plotted coordinates are C---OR, the distance between the O atom of MeOH and the carbene centre atom, and RO---H, the distance between the O and H atoms originating from the MeOH.

Our findings suggest enol formation is the preferred pathway for the reaction of α-carbonyl carbenes with alcohols. This deduction contrasts with the report by Xue *et al.* of direct observation of an alcohol ylide derived from an α-carbonyl carbene.[19] This latter study used a carboethoxy carbene, but our calculations (Figure S13 of Supporting Information) indicate that reactions of such carbenes with an alcohol to form an enol from an ester group remain barrierless. Instead, we propose a structural argument to account for the different experimental observations. The carboethoxy carbene employed by Xue *et al*. can react anti with respect to the carbonyl to form an E-isomer of the ylide which does not have a carbonyl group in the correct orientation for the enol-forming proton transfer reaction. Conjugation of the negative charge of the ylide gives an enolate-like structure which introduces an energy barrier to rotation, therefore preventing rearrangement to the lower-energy enol.[19] In contrast, reactions from both syn and anti faces of the α-carbonyl carbene employed in our experiments offer carbonyl groups in the right orientation to form enols which cannot be spectroscopically distinguished here.

4.4 Singlet carbene

The evidence presented so far of carbene (2) formation is indirectly obtained by monitoring the growth of its reaction products. Direct observation of carbene spectral signatures is complicated by the overlap of spectral features from several species involved in the reactions. However, in ACN we were able to

detect a weak band centred at 1638 cm^{-1} that is in accord with an expected singlet carbene band at 1627 cm^{-1}. The kinetics of the decay of the band match the growth of the ACN ylide band intensity, as shown in Figure 4. Similar observations were made in THF, with a band identified at 1646 cm^{-1} that decays on a timescale consistent with formation of the THF ylide. The shift in the observed wavenumbers of these bands from computational predictions can be explained by solvent-specific interactions at the carbene centre to form an ylidic complex in which there is partial electron donation from the nucleophile to the vacant p-orbital of the carbene centre.[36] Previous reports have identified similar solvent-dependent shifts in the electronic spectra of singlet carbenes.[37]

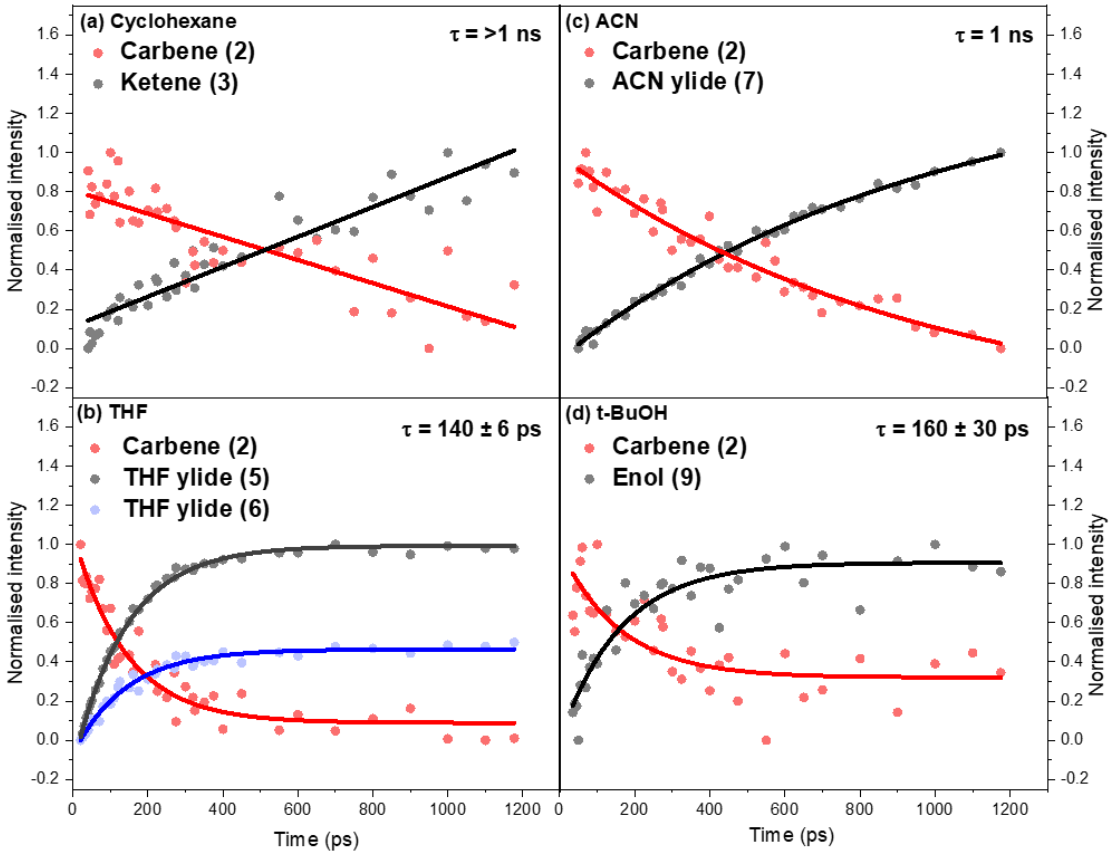

Figure 4 – Kinetics of carbene (2) reactions derived from direct spectroscopic observations following 256-nm excitation of 3.2 mM EDAA solutions. In all panels, normalised intensities for bands assigned to carbene (2) are shown in red, and reaction products are in black or blue. Circles are experimental measurements and solid lines are fits to single exponential functions. (a) decay of the 1620-1650 cm^{-1} band assigned to the carbene (red) and growth of the 1725 cm^{-1} ketene (3) band (black) in cyclohexane. Solid lines are global fits which establish a common exponential time constant of $\tau > 1$ ns. (b) Carbene band decay at 1646 cm^{-1} (red) and growth of the THF ylide (5) band at 1586 cm^{-1} (black) and THF ylide (6) (Blue, $\times 0.5$) (Supporting Information, Table S4, Isomer 4) at 1635 cm^{-1} in THF, $\tau = 140 \pm 6$ ps. (c) Carbene

band decay at 1638 cm^{-1} and growth of the ACN ylide band at 1625 cm^{-1} (black) in ACN τ = 1 ns. (d) Carbene band decay at 1636 cm^{-1}(red) and growth of the enol band at 1694 cm^{-1} (black) in t-BuOH, $\tau = 160 \pm 30$ ps.

The identification and analysis of carbene (2) bands in alcohols is challenging because of the spectral overlap of transient absorption and GSB features in the region where calculations predict a singlet carbene band will appear. However, the slower reaction of the singlet carbene in t-BuOH than in EtOH, evident from the comparative rates of growth of the enol bands, allows separation of the decay of the transient feature centred between 1636 cm^{-1} and the GSB recovery. The decay of the feature in t-BuOH can be fitted to the same time constant as the growth of the enol band (Figure 4(d)), and it may therefore correspond to loss of the singlet carbene.

In cyclohexane, decay of singlet carbene bands should be dominated by the stepwise WR because reaction with solvent is not expected. In accord with this expectation, we see no evidence for carbene insertion into C-H bonds of cyclohexane within the 1.3 ns timescale of our measurements. A weak but prompt growth of an absorption band at 1645 cm^{-1} (Figure 2(a)) could correspond to the singlet carbene but overlaps the wing of a stronger GSB. Its slow decay (Figure 4(a)) is compatible with the stepwise WR route to ketene products.

The prompt formation of bands proposed to arise from singlet carbene (2) in all the different solvents studied supports direct competition between carbene formation and the concerted Wolff rearrangement for photo-excited EDAA. The kinetics of decay of these bands match the growth of products of the stepwise WR and of products of carbene reactions with the solvent. This combination of spectroscopic and kinetic evidence is consistent with carbene (2) being a precursor to stepwise WR reactions, and supports the proposition of competition between this structural rearrangement and bimolecular reaction with solvent molecules.

Conclusion

The UV photoexcitation of ethyl diazo acetoacetate and loss of N_2 leads to ultrafast production of two isomers of a ketene photoproduct via a Wolff rearrangement. The photochemistry also makes a singlet carbonyl carbene intermediate, IR bands of which are identified, and this carbene avoids the rearrangement pathway by rapid reaction with nucleophilic solvents. In tetrahydrofuran or acetonitrile solutions, these reactions produce ylides which are observed via characteristic IR absorption bands at 1586 cm^{-1} and 1625 cm^{-1} respectively. However, in EtOH or t-BuOH, alternative reaction pathways of the singlet carbene are identified. The α-carbonyl group of the carbene influences these O-H insertion reactions by promoting enol formation via a cyclic structure, resembling a pericyclic reaction pathway that

is computed to be barrierless. The enol formation is monitored experimentally via a band at 1694 cm^{-1}. We find no spectroscopic signatures between 1550 cm^{-1} and 1800 cm^{-1} in our measurements of EDAA photochemistry to support a previously proposed alcohol ylide pathway.

Acknowledgements

RP is supported by EPSRC Grant EP/N509619/1. The University of Bristol Ultrafast Laser Laboratory was established with funding from ERC Advanced Grant CAPRI 290966.

Competing interests

The authors declare no competing interests.

Associated content

Supporting information. TRIR spectra and kinetic analysis, UV-vis spectra, FTIR spectra, fitting procedure and computational results

Data are available at the University of Bristol data repository, data.bris, at https://doi.org/10.5523/bris.iqt2f0tmjtut2m0wgxbtsopdo

Correspondence and requests for materials should be addressed to A.J.O.-E.

ORCID

Ryan Phelps : 0000-0001-9036-2133

Andrew Orr-Ewing: 0000-0001-5551-9609

References

1. Simon, R.; Jurij, S.; Branko, S. Ring Contractions of 4-Oxoquinolizine-3-diazonium Tetrafluoroborates, by an Aza Wolff Rearrangement, to Alkyl Indolizine-3-carboxylates. *Eur. J. Org. Chem.* **2001,** *2001*, 3705-3709.
2. Wang, B.; Xie, Y.; Yang, Q.; Zhang, G.; Gu, Z. Total Synthesis of Aquatolide: Wolff Ring Contraction and Late-Stage Nozaki–Hiyama–Kishi Medium-Ring Formation. *Org. Lett.* **2016,** *18*, 5388-5391.
3. Wilds, A. L.; Meader, A. L. The Use of Higher Diazohydrocarbons in the Arndt-Eistert Synthesis. *J. Org. Chem.* **1948,** *13*, 763-779.
4. Burdzinski, G.; Zhang, Y.; Wang, J.; Platz, M. S. Concerted Wolff Rearrangement in Two Simple Acyclic Diazocarbonyl Compounds. *J. Phys. Chem. A* **2010,** *114*, 13065-13068.
5. Wang, J.; Burdzinski, G.; Kubicki, J.; Platz, M. S. Vis and IR Studies of p-Biphenylyl Acetyl and Carbomethoxy Carbenes. *J. Am. Chem. Soc.* **2008,** *130*, 11195-11209.

6. Pecile, C.; Föffani, A.; Ghersetti, S. The Interaction of Diazocarbonyl Compounds with Hydroxylic Solvents. *Tetrahedron* **1964,** *20*, 823-829.
7. Kaplan, F.; Meloy, G. K. The Structure of Diazoketones. A Study of Hindered Internal Rotation1,2. *J. Am. Chem. Soc.* **1966,** *88*, 950-956.
8. Wang, Y.; Yuzawa, T.; Hamaguchi, H.-O.; Toscano, J. P. Time-Resolved IR Studies of 2-Naphthyl(carbomethoxy)carbene: Reactivity and Direct Experimental Estimate of the Singlet/Triplet Energy Gap. *J. Am. Chem. Soc.* **1999,** *121*, 2875-2882.
9. Zhu, Z.; Bally, T.; Stracener, L. L.; McMahon, R. J. Reversible Interconversion between Singlet and Triplet 2-Naphthyl(carbomethoxy)carbene. *J. Am. Chem. Soc.* **1999,** *121*, 2863-2874.
10. Lippert, T.; Koskelo, A.; Stoutland, P. O. Direct Observation of a Photoinduced Wolff Rearrangement in PMMA Using Ultrafast Infrared Spectroscopy. *J. Am. Chem. Soc.* **1996,** *118*, 1551-1552.
11. Wolpert, D.; Schade, M.; Brixner, T. Femtosecond midinfrared study of the photoinduced Wolff rearrangement of diazonaphthoquinone. *J. Chem. Phys.* **2008,** *129*, 094504.
12. Cui, G.; Thiel, W. Photoinduced Ultrafast Wolff Rearrangement: A NonAdiabatic Dynamics Perspective. *Angew. Chem. Int. Ed.* **2013,** *52*, 433-436.
13. Xu, C.; Gu, F. L.; Zhu, C. An excited-state Wolff rearrangement reaction of 5-diazo Meldrum's acid: an ab initio on-the-fly nonadiabatic dynamics simulation. *PCCP* **2018,** *20*, 22681-22688.
14. Ogata, Y.; Sawaki, Y.; Ohno, T. Mechanism for oxidation of phenylacetylenes with peroxymonophosphoric acid. Oxirene as an intermediate inconvertible to ketocarbene. *J. Am. Chem. Soc.* **1982,** *104*, 216-219.
15. Gallucci, R. R.; Jones, M. Photolysis of methyl 3-diazo-2-oxopropionate. Wolff migration of the carbomethoxy group. *J. Org. Chem.* **1985,** *50*, 4404-4405.
16. Maier, G.; Reisenauer, H. P.; Sayrac, T. Oxirene - Intermediate or Transition state - Matrix Irradiation of Diazoketones. *Chem. Ber. Recl.* **1982,** *115*, 2192-2201.
17. Burdzinski, G. T.; Wang, J.; Gustafson, T. L.; Platz, M. S. Study of Concerted and Sequential Photochemical Wolff Rearrangement by Femtosecond UV−vis and IR Spectroscopy. *J. Am. Chem. Soc.* **2008,** *130*, 3746-3747.
18. Naito, I.; Nakamura, K.; Kumagai, T.; Oku, A.; Hori, K.; Matsuda, K.; Iwamura, H. Formation of Nitrile Ylide by Addition of Carbene with Acetonitrile in a Low-Temperature Argon Matrix. *J. Phys. Chem. A* **1999,** *103*, 8187-8192.
19. Xue, J.; Luk, H. L.; Platz, M. S. Direct Observation of a Carbene-Alcohol Ylide. *J. Am. Chem. Soc.* **2011,** *133*, 1763-1765.
20. Hoijemberg, P. A.; Moss, R. A.; Krogh-Jespersen, K. Reversible O-Ylide Formation in Carbene/Ether Reactions. *J. Phys. Chem. A* **2012,** *116*, 358-363.
21. Nuno R. Candeias; Carlos A. M. Afonso Developments in the Photochemistry of Diazo Compounds. *Curr. Org. Chem.* **2009,** *13*, 763-787.
22. Peon, J.; Polshakov, D.; Kohler, B. Solvent Reorganization Controls the Rate of Proton Transfer from Neat Alcohol Solvents to Singlet Diphenylcarbene. *J. Am. Chem. Soc.* **2002,** *124*, 6428-6438.
23. Belt, S. T.; Bohne, C.; Charette, G.; Sugamori, S. E.; Scaiano, J. C. Carbocation Formation via Carbene Protonation Studied by the Technique of Stopped-flow Laser-flash Photolysis. *J. Am. Chem. Soc.* **1993,** *115*, 2200-2205.
24. Kirmse, W. 100 Years of the Wolff Rearrangement. *Eur. J. Org. Chem.* **2002,** *2002*, 2193-2256.
25. Strausz, O. P.; Thap, D. M.; Gunning, H. E. Rearrangement and Polar Reaction of Carbethoxymethylene in 2-Propanol. *J. Am. Chem. Soc.* **1968,** *90*, 1660-1661.
26. Toscano, J. P.; Platz, M. S.; Nikolaev, V.; Popic, V. Carboethoxycarbene. A Laser Flash Photolysis Study. *J. Am. Chem. Soc.* **1994,** *116*, 8146-8151.

27. Chiang, Y.; Jefferson, E. A.; Kresge, A. J.; Popik, V. V.; Xie, R. Q. Conjugate addition of water to acarbonylcarbenes. *J. Phys. Org. Chem.* **1998,** *11*, 610-613.
28. Chiang, Y.; Eustace, S. J.; Jefferson, E. A.; Kresge, A. J.; Popik, V. V.; Xie, R.-Q. Flash photolysis of 4-diazoisochroman-3-one in aqueous solution. Hydration of the carbene produced by loss of nitrogen and ketonization of the enol hydration product. *J. Phys. Org. Chem.* **2000,** *13*, 461-467.
29. Roberts, G. M.; Marroux, H. J. B.; Grubb, M. P.; Ashfold, M. N. R.; Orr-Ewing, A. J. On the Participation of Photoinduced N–H Bond Fission in Aqueous Adenine at 266 and 220 nm: A Combined Ultrafast Transient Electronic and Vibrational Absorption Spectroscopy Study. *J. Phys. Chem. A* **2014,** *118*, 11211-11225.
30. Koyama, D.; Donaldson, P. M.; Orr-Ewing, A. J. Femtosecond to microsecond observation of the photochemical reaction of 1,2-di(quinolin-2-yl)disulfide with methyl methacrylate. *PCCP* **2017,** *19*, 12981-12991.
31. Wiberg, K. B. Basis set effects on calculated geometries: 6-311++G** vs. aug-cc-pVDZ. *J. Comput. Chem.* **2004,** *25*, 1342-1346.
32. Rani, U.; Oturak, H.; Sudha, S.; Sundaraganesan, N. Molecular Structure, Harmonic and Anharmonic Frequency Calculations of 2,4-Dichloropyrimidine and 4,6-Dichloropyrimidine by HF and Density Functional Methods. *Spectrochim. Acta A* **2011,** *78*, 1467-1475.
33. Frey, J. A.; Leist, R.; Tanner, C.; Frey, H.-M.; Leutwyler, S. 2-pyridone: The role of out-of-plane vibrations on the S1↔S0 spectra and S1 state reactivity. *J. Chem. Phys.* **2006,** *125*, 114308-114322.
34. Broda, M. A.; Buczek, A.; Kupka, T.; Kaminsky, J. Anharmonic vibrational frequency calculations for solvated molecules in the B3LYP Kohn–Sham basis set limit. *Vib. Spectrosc* **2012,** *63*, 432-439.
35. Frisch, M. J.; Trucks, G. W.; Schlegel, H. B.; Scuseria, G. E.; Robb, M. A.; Cheeseman, J. R.; Scalmani, G.; Barone, V.; Mennucci, B.; Petersson, G. A.; Nakatsuji, H.; Caricato, M.; Li, X.; Hratchian, H. P.; Izmaylov, A. F.; Bloino, J.; Zheng, G.; Sonnenberg, J. L.; Hada, M.; Ehara, M.; Toyota, K.; Fukuda, R.; Hasegawa, J.; Ishida, M.; Nakajima, T.; Honda, Y.; Kitao, O.; Nakai, H.; Vreven, T.; Montgomery, J. A., Jr.;; Peralta, J. E.; Ogliaro, F.; Bearpark, M.; Heyd, J. J.; Brothers, E.; Kudin, K. N.; Staroverov, V. N.; Kobayashi, R.; Normand, J.; Raghavachari, K.; Rendell, A.; Burant, J. C.; Iyengar, S. S.; Tomasi, J.; Cossi, M.; Rega, N.; Millam, N. J.; Klene, M. K., J. E.;; Cross, J. B.; Bakken, V.; Adamo, C.; Jaramillo, J.; Gomperts, R.; Stratmann, R. E.; Yazyev, O.; Austin, A. J.; Cammi, R.; Pomelli, C.; Ochterski, J. W.; Martin, R. L.; Morokuma, K.; Zakrzewski, V. G.; Voth, G. A.; Salvador, P.; Dannenberg, J. J.; Dapprich, S.; Daniels, A. D.; Farkas, O.; Foresman, J. B.; Ortiz, J. V.; Cioslowski, J.; Fox, D. J. *Gaussian 09, revision D.01*, Gaussian, Inc: Wallingford, CT, 2013.
36. Gómez, S.; Restrepo, A.; Hadad, C. Z. Theoretical tools to distinguish O-ylides from O-ylidic complexes in carbene–solvent interactions. *Physical Chemistry Chemical Physics* **2015,** *17*, 31917-31930.
37. Wang, J.; Kubicki, J.; Gustafson, T. L.; Platz, M. S. The Dynamics of Carbene Solvation: An Ultrafast Study of p-Biphenylyltrifluoromethylcarbene. *J. Am. Chem. Soc.* **2008,** *130*, 2304-2313.

Graphical Abstract